Hyperaldosteronemia and Activation of the Epithelial Sodium Channel Are Not Required for Sodium Retention in Puromycin-Induced Nephrosis

Stéphane Lourdel,* Johannes Loffing,[†] Guillaume Favre,* Marc Paulais,* Antoine Nissant,* Panos Fakitsas,[‡] Christophe Créminon,[§] Eric Féraille,[‖] François Verrey,[‡] Jacques Teulon,* Alain Doucet,* and Georges Deschênes*[¶]

*CNRS/UPMC UMR 7134, IFR 58, Institut des Cordeliers, Paris, France; [†]Department of Medicine, University of Fribourg, Fribourg, Switzerland; [‡]Institute of Physiology, University of Zurich, Zurich, Switzerland; [§]Service de Pharmacologie et d'Immunologie, CEA Saclay, Gif sur Yvette, France; [‖]Fondation pour Recherche Médicale, Geneva, Switzerland; and [¶]Service de Néphrologie Pédiatrique, Hôpital Armand-Trousseau, Paris, France

Edema and ascites in nephrotic syndrome mainly result from increased Na^+ reabsorption along connecting tubules and cortical collecting ducts (CCD). In puromycin aminonucleoside (PAN)-induced nephrosis, increased Na^+ reabsorption is associated with increased activity of the epithelial sodium channel (ENaC) and Na^+,K^+-ATPase, two targets of aldosterone. Because plasma aldosterone increases in PAN-nephrotic rats, the aldosterone dependence of ENaC activation in PAN nephrosis was investigated. For this purpose, (*1*) the mechanism of ENaC activation was compared in nephrotic and sodium-depleted rats, and (*2*) ENaC activity in PAN-nephrotic rats was evaluated in the absence of hyperaldosteronemia. The mechanism of ENaC activation was similar in CCD from nephrotic and sodium-depleted rats, as demonstrated by (*1*) increased number of active ENaC evaluated by patch clamp, (*2*) recruitment of ENaC to the apical membrane determined by immuno-histochemistry, (*3*) shift in the electrophoretic profile of γ-ENaC, and (*4*) increased abundance of β-ENaC mRNA. Corticosteroid clamp fully prevented all PAN-induced changes in ENaC but did not alter the development of a full-blown nephrotic syndrome with massive albuminuria, amiloride-sensitive sodium retention, induction of CCD Na^+,K^+-ATPase, and ascites. It is concluded that in PAN-nephrosis, (*1*) ENaC activation in CCD is secondary to hyperaldosteronemia, (*2*) sodium retention and induction of Na^+,K^+-ATPase in CCD are independent of hyperaldosteronemia, and (*3*) ENaC is not necessarily limiting for sodium reabsorption in the distal nephron.

Interstitial edema observed in nephrotic syndrome results from primary renal Na^+ retention and secondary capillary fluid leakage. In puromycin aminonucleoside (PAN)-induced nephrosis, renal sodium retention mainly originates from connecting tubules and collecting ducts (1). In these nephron segments, Na^+ is reabsorbed by principal cells *via* passive apical entry through amiloride-sensitive epithelium sodium channels (ENaC) and active basolateral extrusion by sodium pumps. In cortical collecting ducts (CCD) of PAN-nephrotic rats, high transepithelial Na^+ transport (2) is associated with activation of ENaC through increased targeting of its α, β, and γ subunits to the apical membrane (3) and *de novo* synthesis and increased targeting of α and β Na^+,K^+-ATPase subunits to the basolateral membrane (4,5). Consistent with these findings, the ENaC inhibitor amiloride fully abolishes

increased sodium transport in *in vitro* microperfused CCD and prevents sodium retention *in vivo* in PAN-nephrotic rats (2).

Aldosterone is the major sodium retaining hormone in the distal tubule. In CCD, aldosterone increases both ENaC and Na^+,K^+-ATPase activities through a biphasic mode: In the short term, it increases the targeting of intracellular pools of ENaC and Na^+,K^+-ATPase to the apical and basolateral membrane, respectively (6,7), and in a later phase, it increases the cellular amount of ENaC and Na^+,K^+-ATPase (8,9). Because plasma aldosterone level is increased in PAN-nephrotic rats at the time of sodium retention (3,10,11), it is usually assumed that hyperaldosteronemia mediates sodium retention in PAN nephrosis. Therefore, we investigated whether activation of ENaC in the CCD during PAN nephrosis is secondary to hyperaldosteronemia.

For this purpose, (*1*) we compared the mechanism of ENaC activation in PAN nephrosis and in sodium restriction–induced hyperaldosteronemia, and (*2*) we evaluated whether ENaC was activated during PAN nephrosis in corticosteroid-clamped rats. Activation of ENaC was assessed through its functional activity, gene expression, subcellular distribution, and electrophoretic mobility of its γ subunit.

Table 1. Conductive properties of ENaC[a]

	G Cell Attached (pS)	E_r (mV)
Adrenal intact		
control	9.6 ± 1.1 (11)	69 ± 17 (11)
PAN nephrosis	10.7 ± 1.1 (8)	40 ± 6 (8)
Na$^+$ depleted	9.5 ± 0.6 (11)	52 ± 5 (11)
Corticosteroid clamped		
control	9.8 ± 1.3 (3)	55 ± 5 (3)
PAN nephrosis	9.7 (1)	82 (1)

[a]Conductive properties of ENaC were determined under cell-attached conditions. ENaC, epithelial sodium channel; G, unitary conductance; Er, apparent reversal potential. Values are means ± SEM from several experiments (number in parenthesis).

Materials and Methods

Animals

Experiments were performed on either normal (adrenal-intact) or corticosteroid-clamped male Sprague-Dawley rats (120 to 130 g). Corticosteroid clamp was achieved by bilateral adrenalectomy and supplementation with 10 μg/kg per d aldosterone and 14 μg/kg per d dexamethasone through subcutaneous osmotic pump (12). Nephrosis was induced by a single injection of PAN (150 mg/kg body wt, intraperitoneally) performed the day after surgery in corticosteroid-clamped

animals. Hyperaldosteronemia was induced in adrenal-intact rats by a single administration of furosemide (200 mg/kg in drinking water) at day 0 followed by a low-sodium diet during 6 d (mean sodium intake 0.25 ± 0.08 mmol/kg body wt per d). All other rats were fed the usual laboratory diet *ad libitum* (mean sodium intake 8.6 ± 0.2 and 6.2 ± 0.9 mmol/kg body wt per d in control and PAN-nephrotic rats, respectively). Nephrotic rats were studied 6 d after PAN administration, when sodium retention and proteinuria were fully developed (13). Sodium-deprived rats were studied 6 d after the onset of the treatment. At that time, their urinary sodium excretion was drastically reduced as compared with control rats: Low-Na$^+$ 4.2 ± 1.3 mmol Na$^+$/mmol creatinine (n = 6); control 24.0 ± 0.5 mmol Na$^+$/mmol creatinine (n = 4).

For metabolic studies, starting 2 d before PAN administration, rats were housed in metabolic cages and 24-h urine was collected for measurement of sodium, creatinine, and proteins. Urinary sodium and protein excretions were calculated as a function of urinary creatinine excretion. The daily urinary sodium balance was calculated as the difference between dietary sodium intake and urinary excretion. Six days after PAN injection, animals were killed for measurement of ascites volume and plasma aldosterone by RIA.

Isolation of Tubules

CCD were dissected from collagenase-treated kidneys as described previously (13). For RNA extraction, tubules were isolated under RNase-free conditions (14), and for patch-clamp and Western blot analysis, antiproteases (PMSF 0.6 mM and leupeptin 0.2 μM) were added to the dissection solution.
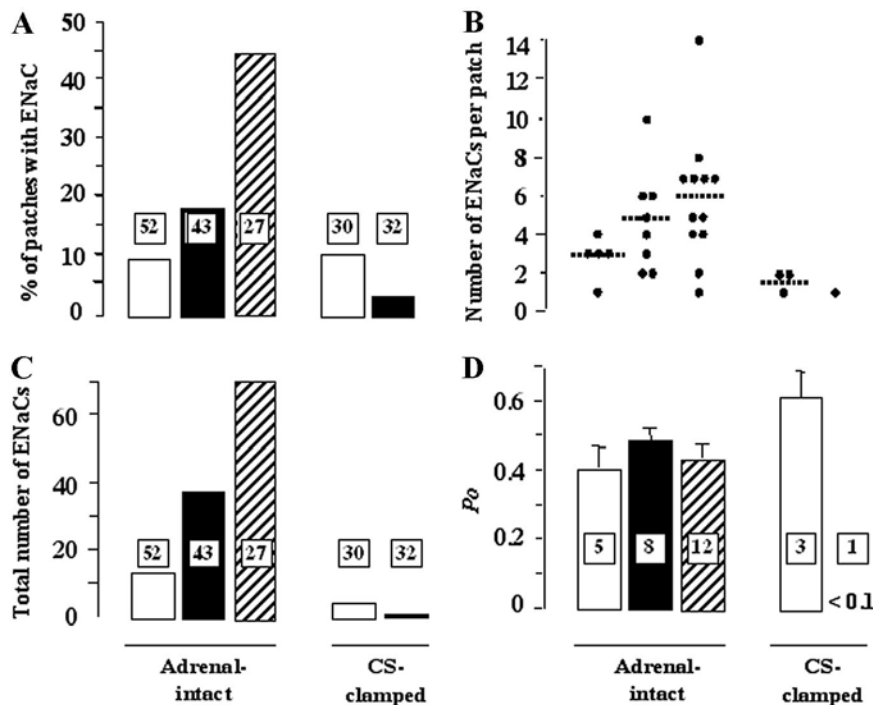

Figure 1. Recording properties of epithelial sodium channel (ENaC) in the cell-attached configuration in cortical collecting ducts (CCD) from adrenal-intact and corticosteroid-clamped rats. (A) Percentage of patches that contained ENaC in CCD from control (□), puromycin aminonucleoside (PAN) nephrotic (■), and Na$^+$-depleted rats (▨) in either adrenal-intact or corticosteroid (CS)-clamped conditions. Values in the columns indicate the total number of patches. (B) Number of channels per patch in the same groups of rats; ●, individual values; dotted lines, mean values. (C) Total number of channels detected throughout the study in the different groups of rats. (D) Open state probability (*Po*) in the five groups; values in columns indicate the number of patches used for determination of *Po*.

Patch-Clamp Recording

Experimental methods were essentially the same as described previously (15). CCD that were placed in a perfusion chamber that was mounted on an inverted microscope were slit-opened manually using a sharpened pipette. The bath solution contained (in mM) 140 NaCl, 4.8 KCl, 1 CaCl$_2$, 1.2 MgCl$_2$, 10 glucose, and 10 HEPES and was adjusted to pH 7.4 with NaOH. The patch pipettes were filled with a solution that contained (in mM) 145 LiCl, 1.2 MgCl$_2$, 10 glucose, and 10 HEPES, adjusted to pH 7.4 with NaOH. Channel activity was measured from digitized stretches of recording lasting at least 30 s. Experiments were carried out at room temperature (22 to 27°C).

Antibodies

Polyclonal antibodies against α, β, and γ subunits of rat ENaC were produced in rabbits (Neosystem, Strasbourg, France) using specific peptides that were described previously (8): NH$_2$-LGKGDKREEQGL-GPEPSAPRQPTC-COOH (amino acids 46 to 68), NH$_2$-CNYDSLRLQ-PLDTMESDSEVEAI-COOH (amino acids 617 to 638), and NH$_2$-CNTL-RLDRAFSSQLTDTQLTNEL-COOH (amino acids 629 to 650) for α-, β-, and γ-ENaC, respectively. Antisera were affinity-purified on EAH-Sepharose 4B (Pharmacia, Paris, France) and eluted with acetate buffer (pH 4) that contained 0.5 M NaCl, formate buffer (pH 3), and finally HCl (pH 1). Acidic fractions were adjusted to pH 7 and immediately completed with Na azide (3 mM) and BSA (500 μg/ml).

Immunoblotting

Kidneys were perfused with ice-cold homogenization solution (250 mM sucrose, 10 mM triethanolamine, 0.6 mM PMSF, and 0.2 μM leupeptin). The cortex was dissected from both kidneys, weighed, and homogenized in 5 vol (vol/wt) of homogenization solution at 0 to 4°C using a Teflon/glass Potter. Protein concentration was adjusted to the same values in all samples with homogenization solution and later controlled with loading gels stained with Coomassie blue.

Samples were solubilized at 60°C for 20 min after addition of 1 vol of 2× Laemmli. SDS-PAGE was performed on 8% polyacrylamide gels. Proteins were electrotransferred to polyvinylidene difluoride membranes (Polyscreen; NEN, Boston, MA), which were stained with Ponceau S solution (Sigma France, Saint Quentin Fallavier, France) to check transfer efficiency among samples. After casein blocking, blots were incubated successively with anti–γ-ENaC antibody (HCl fraction) and goat anti-rabbit IgG antibody coupled to horseradish peroxidase (Promega France, Charbonnières, France) and revealed by chemiluminescence with the Western Lightning Chemiluminescence reagent Plus (PerkinElmer Life Science, Courtabeuf, France). Densitometry of the different bands was quantified by scanning (Image J; National Institutes of Health, Bethesda, MD). Groups of rats were compared by variance analysis; $P < 0.05$ was considered as statistically different.

Immunocytochemistry

After anesthesia, the kidneys of rats ($n = 5$ per group) were perfusion-fixed with 150 ml of fixation solution that contained 3% (wt/vol) paraformaldehyde and 0.05% picric acid, in a 3:2 mixture of 0.1 M cacodylate buffer (pH 7.4, adjusted to 300 mOsmol/kgH$_2$O with sucrose) and 10% hydroxyethyl starch in saline. After a 5-min fixation and a 5-min rinsing period with the cacodylate buffer, the kidneys were removed, sliced, and frozen in liquid propane.
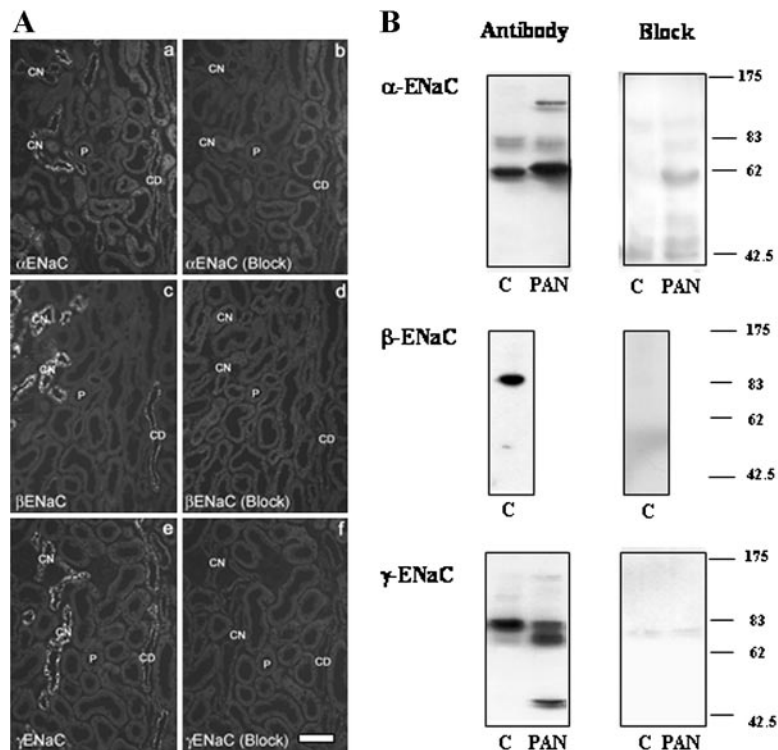

Figure 2. Absorption test for immunofluorescence staining and immunoblots of α-, β-, and γ-ENaC subunits in rat kidney cortex. (A) Kidney cortex sections from control rats were incubated with the antibodies directed against each of the three subunits of ENaC without (a, c, and e) or after preincubation with the immunizing peptide (b, d, and f). P, proximal tubule; CN, connecting tubule located in the cortical labyrinth; CD, cortical collecting duct located in the medullary ray; bar is approximately 100 μm. (B) Immunoblots of kidney cortex homogenates from control (C) and PAN-nephrotic rats (PAN) with antibodies against each of the three subunits of ENaC without (Antibody) or after preincubation with the immunizing peptide (Block).
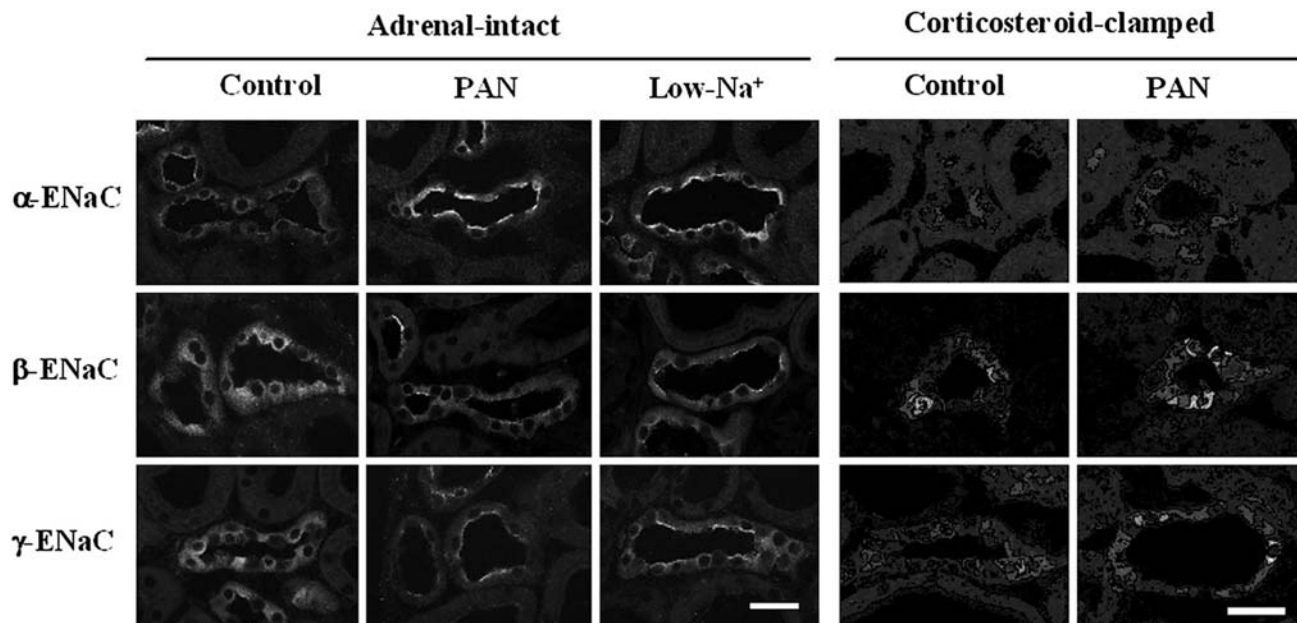
Figure 3. Subcellular localization of α-, β-, and γ-ENaC subunits in connecting tubules (CNT). Indirect immunofluorescent staining of representative CNT profiles for the three subunits of ENaC in control, PAN-nephrotic, and Na$^+$-depleted adrenal-intact and corticosteroid-clamped rats. In adrenal-intact control rats, staining for the three subunits is diffuse within the CNT cells, whereas in both PAN-nephrotic and Na$^+$-depleted rats, the staining is condensed at the apical pole of the CNT cells. In corticosteroid-clamped rats, the staining for all three subunits is diffuse in both control and nephrotic rats. Unstained cells in CNT profiles are intercalated cells. Bar is approximately 40 μm.

Serial 4-μm cryosections were pretreated with 10% normal goat serum in PBS, incubated overnight at 4°C with ENaC antibodies (formate fractions, 1:300), and revealed with a Cy3-conjugated goat anti-rabbit IgG (Jackson Immuno Research Laboratories, West Grove, PA). For each rat, at least five coronal sections of the kidneys were analyzed. Controls of unspecific binding of primary and secondary antibodies were performed by preincubating immune sera with the respective immunogenic peptide or by omitting the primary antibodies.

Real-Time PCR

RNA were extracted from pools of 20 to 50 microdissected CCD according to the technique previously described (14). After purification, RNA were dissolved in 10 μl of water that contained 40 U/ml RNAsin (Promega, Madison, WI). RNA that were extracted from whole kidney cortex using the same protocol served as internal standard for PCR.

Reverse transcription was performed on 8 μl of tubular RNA extract using the first-strand cDNA synthesis kit for reverse transcription–PCR (Roche Diagnostics, Meylan, France), according to the manufacturer's protocol. The remaining 2 μl of RNA extract was processed in parallel in the absence of reverse transcriptase and served as controls (RT^{neg}). Real-time PCR was performed on a LightCycler (Roche Diagnostics) with the LightCycler FastStart DNA Master SYBR Green 1 kit (Roche Diagnostics) according to the manufacturer's protocol, except that the reaction volume was reduced to 8 μl. PCR was performed in the presence of cDNA that corresponded to 0.1 mm of nephron. After PCR, the absence of contaminating PCR products was checked by a fusion curve. No DNA was detectable in RT^{neg} samples and in blanks run in the absence of DNA. In each experiment, a standardization curve was made using serial dilutions (1 to 1:100) of the standard cDNA stock solution made from kidney cortex RNA (dilution 1 corresponded to DNA produced from 16 ng of RNA). For all samples, the amount of PCR product was calculated as percentage of the standard RNA. Re-

sults (arbitrary unit per mm tubule length) are expressed as means ± SEM from several animals. Specific primers (sequences available on request) were designed using ProbeDesign (Roche Diagnostics).

Na$^+$,K$^+$-ATPase Assay

Na$^+$,K$^+$-ATPase activity was determined on pools of four to six permeabilized CCD by the previously described microassay (13). Total ATPase activity was determined in a solution that contained 100 mM NaCl, 5 mM KCl, 10 mM MgCl$_2$, 1 mM EDTA, 100 mM Tris-HCl, 10 mM Na$_2$ATP, and 5 nCi/μl [γ-^{32}P]ATP (Dupont, Boston, MA; 2 to 10 Ci/mmol) at pH 7.4. For Na$^+$,K$^+$-independent ATPase activity measurements, NaCl and KCl were omitted, Tris HCl was 150 mM, and 2 mM ouabain was added. Na$^+$,K$^+$-ATPase activity was taken as the difference between total and Na$^+$,K$^+$-independent ATPase activities.

Results

Aldosterone Status

Plasma aldosterone level was significantly increased in adrenal-intact PAN-nephrotic rats at day 6 (control 661 ± 123 pM, $n = 6$; PAN 3871 ± 240 pM, $n = 7$; $P < 0.001$) but less than in Na$^+$-depleted rats (11773 ± 1757 pM, $n = 9$; $P < 0.001$ *versus* control, $P < 0.025$ *versus* PAN). In corticosteroid-clamped animals, plasma aldosterone was two-fold lower than in control adrenal-intact rats (288 ± 105 pM, $n = 5$; $P < 0.05$ *versus* control adrenal-intact). As expected, PAN treatment no longer increased plasma aldosterone in corticosteroid-clamped rats (283 ± 57, $n = 13$).

Electrical Activity of ENaC

The electrical activity of ENaC was characterized in cell-attached patches by the following criteria: Only inward cur-

rents were observed over the range of potentials tested (-80 to 80 mV); single-channel conductance was in the 6- to 10-pS range in the presence of 145 mM LiCl in the pipette; and the channel kinetics, as estimated qualitatively, were slow (16,17).

The conductive properties of ENaC recorded in adrenal-intact control, PAN-nephrotic, and Na^+-depleted rats were similar in terms of unitary conductance (approximately 10 pS) and apparent reversal potential in cell-attached patches (approximately 55 mV; Table 1). In contrast, the frequency of ENaC was variable between groups (Figure 1). In control CCD, ENaC were detected on five (9.6%) of 52 occasions. Although this disagrees somehow with previous studies that reported no active ENaC in control Na^+-replete rats (18), it is worth noting that the frequency of ENaC remained low and the number of channels per patch was always ≤ 4. As previously reported (18,19), the frequency of patches with ENaC increased greatly in Na^+-depleted rats (12 of 27, 44.4%), and the number of channels per patch was >4 in two of three of the patches. The situation was intermediate in CCD from PAN-nephrotic rats, with 18.6% of patches (eight of 43) that contained ENaC and 50% of the patches with more than four channels. Statistical comparison between control and PAN-nephrotic animals that was assessed by comparing the distribution of the total number of recorded ENaC with an expected equal distribution between the two groups showed a significant difference ($P < 0.001$). The open state probability (Po) was close to 0.4 in the three conditions, fitting with previous findings during hyperaldosteronemia (17–19).

The functional expression of ENaC was not significantly altered by corticosteroid clamp in terms of percentage of patches with ENaC (10 *versus* 9.6% in corticosteroid-clamped *versus* adrenal-intact rats), number of ENaC per patch (1.7 ± 0.6 *versus* 2.8 ± 1.1; Figure 1), and intrinsic properties of ENaC (conductance, reversion potential, and open state probability; Table 1). In corticosteroid-clamped rats, PAN decreased the density of ENaC, as a single channel was detected in 32 (3%) patches. In addition, this channel exhibited a very low Po (<0.1). Given this very low occurrence, we could not determine accurately the properties of this channel, and one might even question whether it was actually an ENaC.

Subcellular Distribution of α-, β-, and γ-ENaC Subunits

Preliminary studies showed that immunostaining by the three antibodies was blocked by preincubation of the antibody with the respective immunogenic peptide (Figure 2). The three subunits of ENaC were detectable in the renal cortex from the three groups of adrenal-intact rats. In normal rats, α-ENaC was predominantly seen in connecting tubules (CNT), and CCD exhibited a very faint immunostaining (Figures 2 and 3), whereas PAN-nephrotic and Na^+-depleted rats displayed intense immunostaining in both CNT and CCD. As previously described (3,8,20), in control rats, α-ENaC immunostaining was weak at the apical membrane, and β- and γ-ENaC were seen predominantly in intracellular compartments. In contrast, in both PAN-nephrotic and Na^+-depleted rats, all three ENaC subunits were well detectable at the apical cell side (Figure 3). As expected from the expression of ENaC in the segment-

specific CNT and CCD cells but not intercalated cells, the three subunits of ENaC were detected in a subset of the epithelial cells that line the CNT and CCD in the three groups of rats. In corticosteroid-clamped rats, immunohistochemistry confirmed the lack of activation of ENaC in the distal nephron of PAN-treated rats, as the immunostaining for ENaC remained faint and mainly intracellular for all three subunits (Figure 3).

Expression of α-, β-, and γ-ENaC mRNA

Na^+ depletion increased the abundance of α- and β- but not γ-ENaC mRNA (Figure 4). PAN nephrosis induced qualitatively similar effects on ENaC mRNA, although increase in α-ENaC mRNA did not reach statistical significance. Expression of ENaC mRNA was no longer increased in corticosteroid-clamped PAN-nephrotic rats (Figure 4). Corticosteroid clamp also prevented the increase in serum- and glucocorticoid-induced kinase (sgk) mRNA observed in adrenal-intact nephrotic and Na^+-depleted rats (Figure 4).

Electrophoretic Mobility of γ-ENaC

In Western blot of kidney cortex from adrenal intact rats, anti–γ-ENaC stained two main bands of approximately 83 and
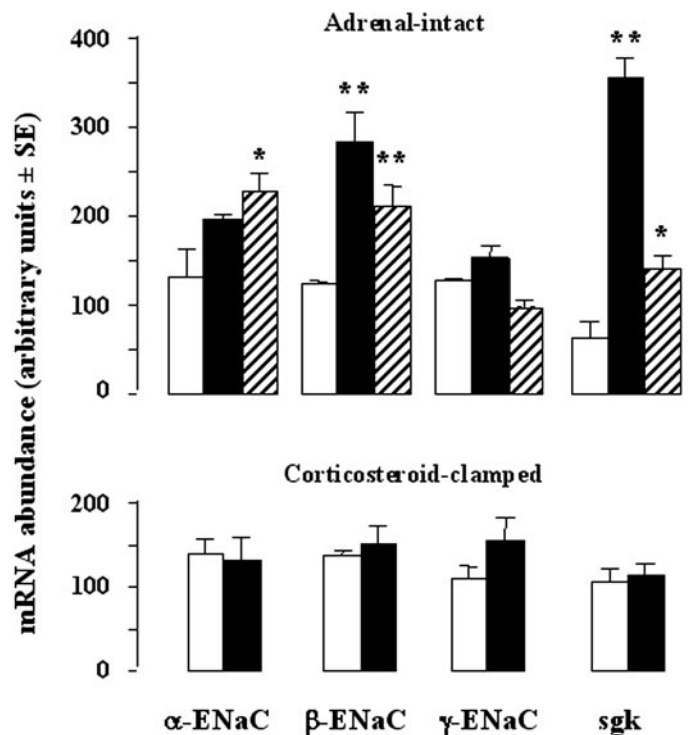
Figure 4. Expression of α-, β-, and γ-ENaC and sgk mRNA in CCD from adrenal-intact and corticosteroid-clamped rats. Expression of mRNA encoding the three subunits of ENaC and sgk was determined by reverse transcription followed by real-time PCR on CCD dissected from control (□), PAN-nephrotic (■), or Na^+-depleted rats (▨). For all samples, the amount of PCR product was calculated as percentage of the standard RNA. Results (arbitrary unit per mm tubule length) are expressed as means $\pm$ SEM from five to 11 animals. Values that were statistically different from controls were determined by variance analysis: *$P < 0.05$; **$P < 0.005$. Note that comparison of expression levels of two different transcripts is meaningless.
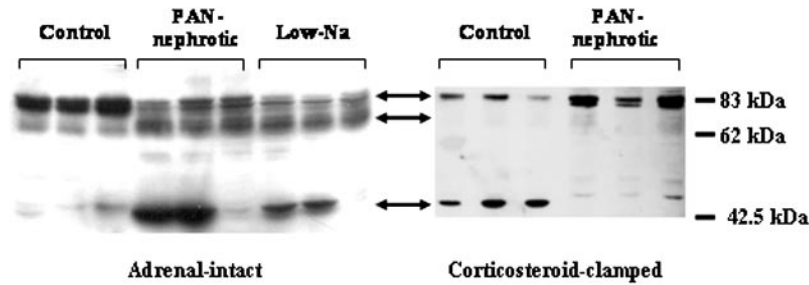
Figure 5. Immunoblots of γ-ENaC subunits in kidney cortex from adrenal-intact and corticosteroid-clamped rats. The figure shows two representative immunoblots with three animals from each group. In adrenal-intact rats, PAN nephrosis and Na$^+$ depletion induce a shift of the migration profile with decreased and increased density of the 83- and 70-kD bands, respectively. In corticosteroid-clamped rats, the 70-kD band was not detectable in both control and nephrotic rats. Note that an additional band migrating at approximately 50-kD band was detected in some animals from all groups.

70 kD in the three groups of rats (Figure 5). As previously reported (3,8), the density ratio of the 83-/70-kD bands was significantly decreased in PAN-nephrotic and Na$^+$-depleted rats as compared with controls (mean ± SEM, $n = 6$ in each group; control 4.18 ± 0.58; PAN-nephrotic 1.09 ± 0.18, $P < 0.001$; low-Na$^+$ 0.68 ± 0.07, $P < 0.001$). In corticosteroid-clamped rats, the 70-kD band was undetectable in all six rats of the control and PAN-treated groups. In the five groups of rats, an additional low molecular weight (approximately 50 kD) band was detected in some but not all rats. All signals that were detected by the anti–γ-ENaC antibody disappeared when the antibody was preincubated with the immunogenic peptide (Figure 2).

Renal Handling of Sodium

PAN-induced changes in the profile of sodium excretion and sodium balance were similar in adrenal-intact and corticosteroid-clamped rats except at day 2, when both parameters were normal in the latter group (Figure 6). In both adrenal-intact and corticosteroid-clamped rats, proteinuria appeared at day 4 after PAN administration and rose rapidly up to day 6.

At day 6, adrenal-intact and corticosteroid-clamped PAN-nephrotic rats displayed similar volumes of ascites ranging 1 to 14 ml (mean ± SEM 6.0 ± 2.0 ml; $n = 7$) and 1 to 12 ml (mean ± SEM 6.0 ± 1.0; $n = 13$) in the two groups, respectively. In adrenal-intact rats, there was no correlation between the volume of ascites and the plasma aldosterone level at day 6.

Mechanism of Sodium Retention in Corticosteroid-Clamped Nephrotic Rats

The absence of ENaC activation in CCD of corticosteroid-clamped nephrotic rats raises the questions of the site and cellular mechanism of sodium retention in these rats. In corticosteroid-clamped nephrotic rats, Na$^+$,K$^+$-ATPase activity was increased in the CCD (Figure 7), as previously observed in adrenal-intact rats (13). Also, PAN nephrosis increased the expression of Na$^+$,K$^+$-ATPase α_1 subunit mRNA in CCD from adrenal-intact and corticosteroid-clamped rats (Figure 8). Finally, within 1 d, amiloride treatment (1 mg/kg per d) fully reversed PAN-induced sodium retention (Figure 9) and ascites in corticosteroid-clamped

rats. Altogether, these results indicate that in both adrenal-intact and corticosteroid-clamped nephrotic rats, sodium retention originates at least in part from the collecting duct and
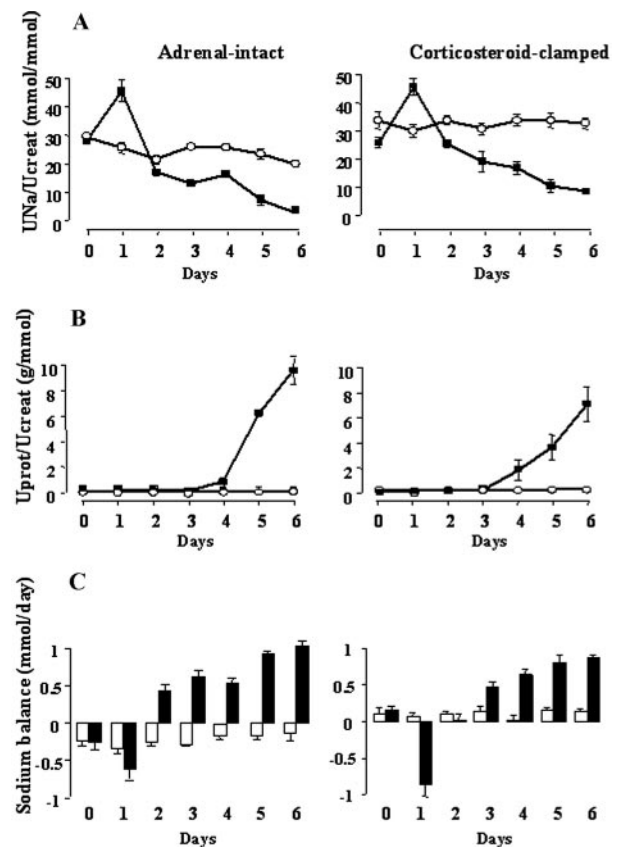

Figure 6. Renal excretion of sodium and protein and sodium balance in the early phase of PAN nephrosis in adrenal-intact and corticosteroid-clamped rats. Time course of 24-h urinary Na$^+$ excretion (A), protein excretion (B), and Na$^+$ balance (C) in adrenal-intact and corticosteroid-clamped rats after a single injection of PAN at day 0 (● and ■) or controls (○ and □). Results at day 0 correspond to the 24-h urine sample collected the day before PAN injection. Na$^+$ and protein excretion are normalized to creatinine excretion. Values are means ± SEM from five rats.
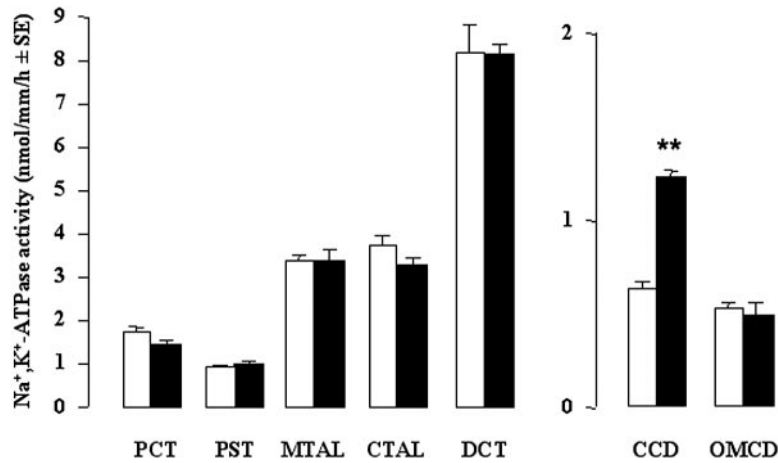
Figure 7. Na$^+$,K$^+$-ATPase activity along the nephron of corticosteroid-clamped rats. Na$^+$,K$^+$-ATPase activity was determined in the different segments of nephron of control rats (□) and rats that received an injection of PAN 6 d before the experiment (■). Values are means ± SEM from five control and four nephrotic rats. Values that were statistically different from controls were determined by *t* test for unpaired data: **$P < 0.001$.
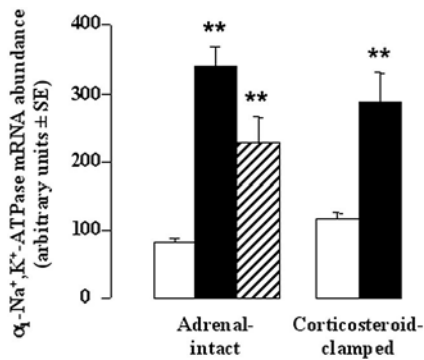

Figure 8. Expression of Na$^+$,K$^+$-ATPase mRNA in CCD from adrenal-intact and corticosteroid-clamped rats. Expression of mRNA encoding Na$^+$,K$^+$-ATPase α_1 subunit was determined by reverse transcription followed by real-time PCR on CCD that were dissected from control (□), PAN-nephrotic (■), or Na$^+$-depleted rats (▨). For all samples, the amount of PCR product was calculated as percentage of the standard RNA. Results (arbitrary unit per mm tubule length) are expressed as means ± SEM from five to 10 animals. Values that were statistically different from controls were determined by variance analysis: **$P < 0.001$.

is accounted for primarily by induction of Na$^+$,K$^+$-ATPase. It is worth noting that corticosteroid-clamped rats were much more sensitive to amiloride than adrenal-intact rats: At the dose of 20 mg/kg per d amiloride used in our previous study in adrenal-intact PAN-treated rats (2), all corticosteroid-clamped nephrotic rats died within 48 h with symptoms of severe volume contraction.

Discussion

Our results confirm the previously reported activation of kidney ENaC in PAN nephrosis (3) and further document its mechanism. In PAN-nephrosis, ENaC was activated in CCD by the same mechanism as in hyperaldosteronemia: In both con-

ditions, the functional activity of ENaC was increased in CCD without change of its intrinsic properties. Increased ENaC activity was accounted for by the recruitment of intracellular ENaC to the apical membrane. Whether membrane recruitment of ENaC is associated with *de novo* synthesis of channel units remains difficult to address *in vivo*, in the absence of protein metabolic labeling. At variance with a previous report (11), our results show an increased level of β-ENaC mRNA in CCD from PAN-nephrotic rats. At the protein level, there are also discrepancies in the literature as Audigé *et al.* (11) reported increased amounts of α-ENaC and no change in β- and γ-ENaC in the kidney cortex of PAN-nephrotic rats, whereas Kim *et al.* (3) described no change in α- and β-ENaC abundance and an increase of γ-ENaC. From these data, it can be concluded that recruitment of pre-existing ENaC is the main cause of increased ENaC activity in PAN nephrosis.

Altogether, these findings suggest that hyperaldosteronemia accounts for the stimulation of ENaC in PAN nephrosis. This conclusion was fully confirmed by the finding that preventing hyperaldosteronemia in PAN-nephrotic rats by corticosteroid clamp prevented the activation of ENaC and its recruitment to the apical membrane. It is interesting that there was a linear correlation between plasma aldosterone level and the density of ENaC in the apical membrane (Figure 10). In contrast, the correlation between plasma aldosterone and sgk mRNA was weak (Figure 10), suggesting that aldosterone-induced recruitment of ENaC may be accounted for only in part by induction of sgk.

Recruitment of intracellular ENaC to the apical membrane is associated with a change in the electrophoretic profile of γ-ENaC, in both hyperaldosteronemia (8) and PAN nephrosis (3). Our results confirm these findings, as the relative abundance of the 70-kD form of γ-ENaC increased at the expense of the 83-kD form. Again, there was a good correlation between plasma aldosterone level and the molecular weight shift of
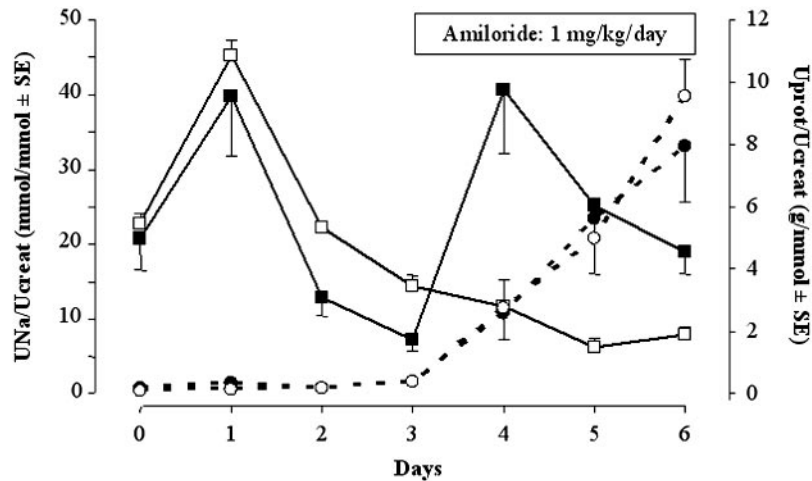
Figure 9. Effect of amiloride on urinary sodium excretion in corticosteroid-clamped PAN-nephrotic rats. Time course of 24-h urinary Na^+ and protein excretion (solid and dotted lines, respectively) in corticosteroid-clamped rats after a single injection of PAN at day 0. Results at day 0 correspond to the 24-h urine sample collected the day before PAN injection. Starting after the fourth 24-h urine collection, part of the rats received amiloride (1 mg/kg per d) in the food (●, ■). Na^+ and protein excretion are normalized to creatinine excretion. Values are means ± SEM from five rats.
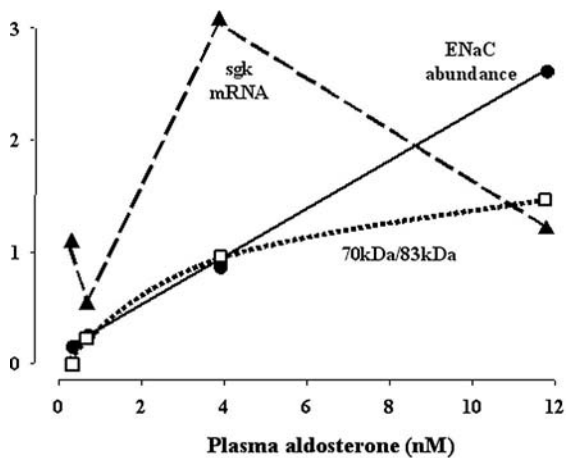

Figure 10. Correlations between plasma aldosterone level and expression of sgk mRNA, ENaC abundance, and shift in molecular weight of γ-ENaC in different groups of rats. This figure summarizes data corresponding to the three groups of adrenal-intact rats and control corticosteroid-clamped rats. Data for sgk mRNA expression (pecked line, arbitrary units) are from Figure 4. ENaC abundance (solid line, absolute values) was calculated as the ratio between the total number of channels detected by patch clamp and the total number of patches. The shift in γ-ENaC molecular weight (dotted line, absolute values) was calculated as the mean density ratio of the 70-/83-kD bands. Results for ENaC abundance and shift in γ-ENaC molecular weight were fitted using SigmaPlot to linear ($r^2 = 0.999$) and Michaelis plot ($r^2 = 0.997$), respectively, whereas data for sgk mRNA expression did not fit satisfactorily to any usual plot.

γ-ENaC, although some saturation appeared at high aldosterone concentration (Figure 10).

In aldosterone-clamped rats, PAN treatment not only failed to recruit ENaC to the apical membrane but also altered the Po

of pre-existing ENaC. Such a change in Po, which probably reflects partial degradation of the channels, was induced by PAN and not by corticosteroid clamp *per se* and was not seen in adrenal-intact rats. This decrease in Po is likely accounted for by a toxic effect of PAN also revealed by the transient increase in sodium excretion and decrease in Na^+,K^+-ATPase activity (13) observed at day 1. A transient degradation of ENaC present in apical membranes can be rapidly compensated by recruitment of nondegraded intracellular ENaC in adrenal-intact animals but not in corticosteroid-clamped ones. Partial degradation of ENaC may also account for (*1*) the decreased abundance of functional channels and (*2*) the high amiloride sensitivity observed in corticosteroid-clamped, PAN-nephrotic animals.

In contrast, corticosteroid clamp did not prevent PAN-induced stimulation of Na^+,K^+-ATPase in CCD. In addition, as previously demonstrated in adrenal-intact rats, this stimulation is accounted for by *de novo* synthesis of the pump. These findings confirm previous reports of increased Na^+,K^+-ATPase activity in CCD of adrenalectomized PAN-nephrotic rats (4). They also indicate that induction of Na^+,K^+-ATPase in PAN nephrosis is independent not only of aldosterone but also of sgk, the induction of which was prevented in corticosteroid-clamped rats. The signaling mechanism linking Na^+,K^+-AT-Pase induction and PAN nephrosis remains to be elucidated.

The most striking result of this study was that, in corticosteroid-clamped rats, PAN continued to induce amiloride-sensitive retention of sodium despite the decreased number and Po of ENaC, indicating that induction of Na^+,K^+-ATPase is sufficient to increase sodium reabsorption. This means that increased activity of Na^+,K^+-ATPase at the basolateral pole of the cells is able to reduce sufficiently the intracellular sodium concentration so as to generate a driving force across the apical membrane sufficient to compensate its markedly reduced conductance to sodium. With this regard, it is noticeable that Na^+,K^+-ATPase in CCD displays a very high affinity for so-

8

dium (21), therefore allowing the maintenance of a high activity at low intracellular sodium concentration. This demonstrates that in such circumstances, apical ENaC is far from being the rate-limiting step of sodium reabsorption in CCD. Such a conclusion was recently reached in mouse CCD in response to $ERK_{1,2}$ activation (22).

In conclusion, at the time of renal sodium retention and ascites, PAN-nephrotic rats exhibit increased apical ENaC activity that results from hyperaldosteronemia-induced recruitment of an intracellular pool of channels. However, activation of ENaC appears as an epiphenomenon that is not necessary for full activation of transepithelial sodium reabsorption, as long as some residual ENaC activity remains in the apical membrane.

References

1. Ichikawa I, Rennke HG, Hoyer JR, Badr KF, Schor N, Troy JL, Lechene CP, Brenner BM: Role for intrarenal mechanisms in the impaired salt excretion of experimental nephrotic syndrome. *J Clin Invest* 71: 91–103, 1983

2. Deschenes G, Wittner M, Stefano A, Jounier S, Doucet A: Collecting duct is a site of sodium retention in PAN nephrosis: A rationale for amiloride therapy. *J Am Soc Nephrol* 12: 598–601, 2001

3. Kim SW, Wang W, Nielsen J, Praetorius J, Kwon TH, Knepper MA, Frokiaer J, Nielsen S: Increased expression and apical targeting of renal ENaC subunits in puromycin aminonucleoside-induced nephrotic syndrome in rats. *Am J Physiol Renal Physiol* 286: F922–F935, 2004

4. Vogt B, Favre H: Na+,K(+)-ATPase activity and hormones in single nephron segments from nephrotic rats. *Clin Sci (Lond)* 80: 599–604, 1991

5. Deschenes G, Gonin S, Zolty E, Cheval L, Rousselot M, Martin PY, Verbavatz JM, Feraille E, Doucet A: Increased synthesis and AVP unresponsiveness of Na,K-ATPase in collecting duct from nephrotic rats. *J Am Soc Nephrol* 12: 2241–2252, 2001

6. Summa V, Mordasini D, Roger F, Bens M, Martin PY, Vandewalle A, Verrey F, Feraille E: Short term effect of aldosterone on Na,K-ATPase cell surface expression in kidney collecting duct cells. *J Biol Chem* 276: 47087–47093, 2001

7. Loffing J, Zecevic M, Feraille E, Kaissling B, Asher C, Rossier BC, Firestone GL, Pearce D, Verrey F: Aldosterone induces rapid apical translocation of ENaC in early portion of renal collecting system: Possible role of SGK. *Am J Physiol Renal Physiol* 280: F675–F682, 2001

8. Masilamani S, Kim GH, Mitchell C, Wade JB, Knepper MA: Aldosterone-mediated regulation of ENaC alpha, beta, and gamma subunit proteins in rat kidney. *J Clin Invest* 104: R19–R23, 1999

9. Welling PA, Caplan M, Sutters M, Giebisch G: Aldosterone-mediated Na/K-ATPase expression is alpha 1 isoform specific in the renal cortical collecting duct. *J Biol Chem* 268: 23469–23476, 1993

10. Pedraza-Chaverri J, Cruz C, Ibarra-Rubio ME, Chavez MT, Calleja C, Tapia E, del Carmen Uribe M, Romero L, Pena JC: Pathophysiology of experimental nephrotic syndrome induced by puromycin aminonucleoside in rats. I. The role of proteinuria, hypoproteinemia, and renin-angiotensin-aldosterone system on sodium retention. *Rev Invest Clin* 42: 29–38, 1990

11. Audige A, Yu ZR, Frey BM, Uehlinger DE, Frey FJ, Vogt B: Epithelial sodium channel (ENaC) subunit mRNA and protein expression in rats with puromycin aminonucleoside-induced nephrotic syndrome. *Clin Sci (Lond)* 104: 389–395, 2003

12. Khadouri C, Marsy S, Barlet-Bas C, Cheval L, Doucet A: Effect of metabolic acidosis and alkalosis on NEM-sensitive ATPase in rat nephron segments. *Am J Physiol* 262: F583–F590, 1992

13. Deschenes G, Doucet A: Collecting duct (Na+/K+)-ATPase activity is correlated with urinary sodium excretion in rat nephrotic syndromes. *J Am Soc Nephrol* 11: 604–615, 2000

14. Elalouf JM, Buhler JM, Tessiot C, Bellanger AC, Dublineau I, de Rouffignac C: Predominant expression of beta 1-adrenergic receptor in the thick ascending limb of rat kidney. Absolute mRNA quantitation by reverse transcription and polymerase chain reaction. *J Clin Invest* 91: 264–272, 1993

15. Lourdel S, Paulais M, Cluzeaud F, Bens M, Tanemoto M, Kurachi Y, Vandewalle A, Teulon J: An inward rectifier K(+) channel at the basolateral membrane of the mouse distal convoluted tubule: Similarities with Kir4-Kir5.1 heteromeric channels. *J Physiol* 538: 391–404, 2002

16. Palmer LG, Frindt G: Effects of cell Ca and pH on Na channels from rat cortical collecting tubule. *Am J Physiol* 253: F333–F339, 1987

17. Palmer LG, Frindt G: Amiloride-sensitive Na channels from the apical membrane of the rat cortical collecting tubule. *Proc Natl Acad Sci U S A* 83: 2767–2770, 1986

18. Pacha J, Frindt G, Antonian L, Silver RB, Palmer LG: Regulation of Na channels of the rat cortical collecting tubule by aldosterone. *J Gen Physiol* 102: 25–42, 1993

19. Lu M, Giebisch G, Wang W: Nitric oxide-induced hyperpolarization stimulates low-conductance Na+ channel of rat CCD. *Am J Physiol* 272: F498–F504, 1997

20. Loffing J, Pietri L, Aregger F, Bloch-Faure M, Ziegler U, Meneton P, Rossier BC, Kaissling B: Differential subcellular localization of ENaC subunits in mouse kidney in response to high- and low-Na diets. *Am J Physiol Renal Physiol* 279: F252–F258, 2000

21. Barlet-Bas C, Cheval L, Khadouri C, Marsy S, Doucet A: Difference in the Na affinity of Na(+)-K(+)-ATPase along the rabbit nephron: Modulation by K. *Am J Physiol* 259: F246–F250, 1990

22. Michlig S, Mercier A, Doucet A, Schild L, Horisberger JD, Rossier BC, Firsov D: ERK1/2 controls Na,K-ATPase activity and transepithelial sodium transport in the principal cell of the cortical collecting duct of the mouse kidney. *J Biol Chem* 279: 51002–51012, 2004